King Saud University

Arabian Journal of Chemistry

www.ksu.edu.sa
www.sciencedirect.com

ORIGINAL ARTICLE

Comprehensive study on saline-alkali soil amelioration with sediment of irrigation area in northeast China

Yuyan Zhao, Zeyu Zhang, Zhenghe Li, Binghan Yang, Bing Li, Xiaodan Tang [*], **Yawen Lai**

College of Geo-exploration Science and Technology, Jilin University, Changchun 130026, China

Abstract To improve the main shortcomings of insufficient nutrients, high salinity and low productivity in saline-alkali soils, this study collected saline-alkali soil samples from Da'an City of Baicheng and sediment samples from the adjacent Qianguo irrigation district, measured their pH values and major element contents, designed and verified the improvement scheme of saline-alkali soil based on geochemical engineering principles. Results indicated that the pH value and various element contents of saline-alkali soil could be adjusted by adding sediment to make it close to reference soil. Both theoretical calculation and experimental determination (soil pH, mineral composition, functional group composition and crop growth) revealed that the optimal mixing ratio of saline-alkali soil and sediment was 2:1. The saline-alkali soil amelioration with sediment of adjacent irrigation areas was effectively, low-cost and environment-friendly. The geochemical engineering principle was applicable to the amelioration of saline-alkali soil, but the mixing ratio of saline-alkali soil and sediment in different areas should vary with the local conditions. Meanwhile, theoretical calculation could basically replace the experimental determination to simplify the actual engineering application process. This saline-alkaline soil amelioration method makes full use of the surrounding natural waste and has the advantage of adapting measures to local conditions.
© 2023 The Authors. Published by Elsevier B.V. on behalf of King Saud University. This is an open access article under the CC BY-NC-ND license (http://creativecommons.org/licenses/by-nc-nd/4.0/).
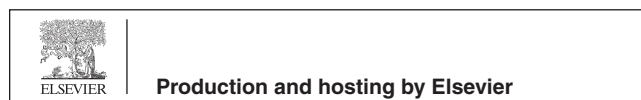
1. Introduction

Soil salinity is the key factor restricting the production on part of cropland (Li et al., 2020; Qadir et al., 2008). The crop productivity on 25% of the world's irrigated land has been reduced because of the excessive salt (Mao et al., 2016; Wong et al., 2010). As the world's population increases and living standards improve, more land is needed to produce crops to meet human needs (Bouwer, 2000). Thus, it is quite necessary for the remediation of saline-alkali land to enable unproductive land for agricultural production. China is a populous agricultural

* Corresponding author.
 E-mail address: tangxiaodan@jlu.edu.cn (X. Tang).
Peer review under responsibility of King Saud University.

Production and hosting by Elsevier

country. The security of arable land and food is of great strategic significance in the development of national economy. The quality of cultivated land is one of the important indictors of agricultural comprehensive production capacity. However, in the 1960s and 1970s, due to the fast population growth, cultivated land demand increased rapidly in China, large numbers of forests, grasslands, wetlands and other lands were reclaimed as cultivated land (Guo et al., 2010). The intensity of land use increased sharply, original vegetation and soil structure were destroyed, and land degradation, including salinization, occurred in a large area (Fu et al., 2018). Today, China and even the whole world are facing population-environment-resource problems (Amini et al., 2016). Soil erosion, land desertification and salinization are becoming more and more serious (Zhu et al., 2021). Soil salinization is one of the main reasons for soil degradation, land resource shortage and ecological environment deterioration. The saline-alkali soil of China is distributed in plains, basins and coastal areas of 23 provinces, municipalities and autonomous regions, covering an area of about 36 million hectares (Wang et al., 2021a, 2021b). The direct economic losses caused by soil salinization are up to 2.5 billion yuan per year, which adversely affects the country's economic prosperity (Bao et al., 2016; Jonathan et al., 2018). Improving saline-alkali land and its ecological environment is conducive to achieving sustainable economic development and ensuring national food security (Kuzmin et al., 2020; Yang et al., 2021a). With a growing population and a shrinking arable land area, it is urgent to improve and utilize saline-alkali land to keep the red line of "1.8 billion mu of arable land nationwide".

For saline-alkali soil, its salt content is generally between 0.1 % and 0.2 %, and its pH is greater than 9. The components with excessive content are mainly four anions (CO_3^{2-}, HCO_3^-, Cl^-, SO_4^{2-}) and four cations (Ca^{2+}, Mg^{2+}, K^+, Na^+) (Li et al., 2018). High concentrations of these ions have a negative impact on ecosystem biodiversity, crop yields, public health, urban and rural infrastructure (Rahneshan et al., 2018; Zhang et al., 2018). In addition, the lack of nutrient elements and the enrichment of some non-essential heavy metals in saline-alkali soil will also restrict the plant growth (Evgeny et al., 2021; Yang et al., 2019).

At present, the world-recognized improvement methods for saline-alkali soil include water conservancy engineering and agricultural remediation, chemical and biological methods, etc. (Zhao et al., 2018). In China, Ge et al. (2018) took mulching measures to improve soil bulk density and organic matter content; Li et al. (2020) repaired the physical and chemical properties of saline soil by organic and inorganic remediation agents. Pakistan had undertaken large-scale salinity control and reclamation project through hydro-engineering and agricultural remediation, which covered 8 million hm^2 of soil at an estimated cost of $2 billion. However, the characteristics of saline-alkali soil (complex formation, numerous types, uncontrollability) made the various remediation methods complicated, time-consuming and costly (Wang et al., 2021a). So, it is necessary to use materials according to the local conditions and establish a green improvement technology with low price, simple operation and obvious effect to modify the saline-alkali soil quality.

Geochemical engineering is an emerging branch of geochemistry at the end of last century (Schuiling, 1998). It generally has the advantages of low cost, small energy consumption, no dependence on high-tech equipment, and conversion an environmental problem into a commercial commodity (Wu, 2002). This makes geochemical engineering have a broad prospect in environmental remediation and pollution control (Schuiling, 1990). For example, in the Klivorog iron mine area of Ukraine, the mine water containing three times the salinity of sea water was concentrated and crystallized into salt for use by taking advantage of the local natural conditions. The Armyansk Chemical Factory in Crimea reacted the waste acid discharged every year with the carbonate rocks at the bottom of the shallow bay to form an isolation layer to prevent the acid from infiltrating and polluting the groundwater (Wu, 2002). Therefore, if the principle of geochemical engineering is applied to the saline-alkali soil amelioration, it will provide a low-cost green technology for the restoration and reconstruction of regional ecosystem functions.

The saline-alkali land of Songnen Plain was about 2.4×10^6 hm^2 (mostly lightly salinized reed marshes and almost no alkalized soil) in 1950 and increased to 3.2×10^6 hm^2 by 1990 and 3.94×10^6 hm^2 by 2016. With the change of natural environment and the influence of human activities, the area of heavily salinized land is increasing (Yang et al., 2021b). What's more, the western part of Jilin province is an important grain producing area in China (Wang et al., 2018; Zhang et al., 2010). In recent years, due to land consolidation, paddy fields had been obviously increased and many large irrigated areas had been developed (Pu et al., 2018). As a result, the internal structure of cultivated land had undergone drastic changes, and a large amount of sediment had accumulated in the irrigated areas (Yang et al., 2014). These sediments, rich in organic matter, nitrogen (N), phosphorus (P) and mineral elements, have the value of improving soil fertility. Therefore, the west of Jilin province was selected as experimental research area, and the saline-alkali soil in the area was ameliorated with the sediment in backwater channels of adjacent irrigated area based on the principle of geochemical engineering. The purpose of this study is to construct a new idea for the amelioration and restoration of saline-alkali land, and to verify whether theoretical calculations can replace batch experiments to simplify subsequent practical engineering applications.

2. Materials and methods

2.1. Study areas and sample processing

The pilot site was chosen in Baicheng, in western Jilin province, China. This area is the west extension zone of Songnen Plain, a transition zone from humid climate to arid climate, and a famous salinized land distribution area in China. With the influence of neotectonic activities, the mountainous area around Songnen Plain has formed the igneous rock area with wide distribution and relatively large alkaline mineral composition (Bian et al., 2012). Under the long-term external force, it provides direct salt source for the plain. The influence of neotectonic activities also extends to plain topography, water system, etc. On the whole, the topography is high in the east and low in the west, which changes the water runoff path, promotes the subsidence center of the basin to migrate westward, and eventually forms a closed flow zone of salt accumulation (Wang, 1993). The climate of Baicheng is characterized by large evaporation capacity and high wind speed. The ratio of evaporation capacity to rainfall is above 4 all the year round. In addition, excessive irrigation and blind grazing led to the increase of soil salinization in the study area.

Through preliminary data collection and field exploration, the saline-alkali soils (N45°23′54″, E124°6′21″) in Da'an City of Baicheng and the sediments of its adjacent backwater channels in Qianguo irrigation district (N45°21′42″, E124°19′4″) (shown in Fig. 1) were selected and collected for the study. Qianguo irrigated area is rich in sediment resources, and the transport distance between two points is within 50 km, which satisfies the requirements of lower transport costs. In addition, the reference soil (N44°34′56″, E126°46′49″) was collected from Yushu City which can ensure the normal growth and development of plants. All the above samples were air-dried and passed through 10 mesh (< 2mm) screen.
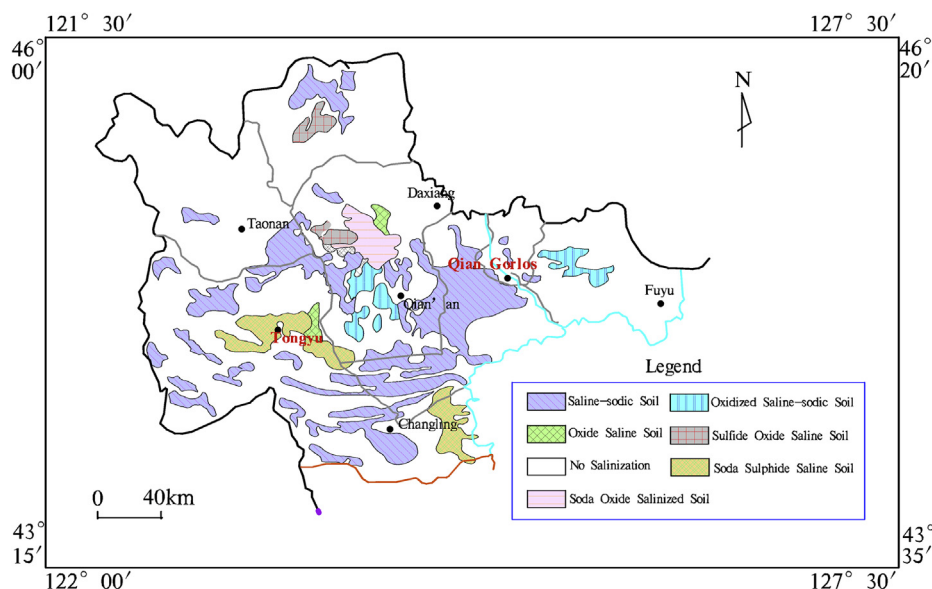
Fig. 1   Distribution map of salinization in western Jilin.

2.2. Reagents and standards

Hydrochloric acid (HCl), boric acid (H_3BO_3), sulfuric acid (H_2SO_4), sodium thiosulfate pentahydrate ($NaS_2O_3 \cdot 5H_2O$), ferrisulphas ($FeSO_4 \cdot 7H_2O$), monopotassium phosphate (KH_2PO_4) and sodium hydroxide (NaOH) in guaranteed reagent grade and ultrapure deionized water with a resistivity of 18.2 MΩ cm at 25 ℃ were used for sample preparation. The other reagents were of analytical grade. The main reagents prepared in the experiment were 42 g/L sodium bicarbonate, molybdenum-antimony chromogenic agent (the mixed solution of 0.5 g ascorbic acid, 5 mL 3 g/L antimony potassium tartrate and 95 mL 5 g/L ammonium molybdate), 2 g/L 2,4-dinitrophenol indicator, molybdate solution (the mixed solution of 300 mL H_2SO_4, 100 mL 3.5 g/L antimony potassium tartrate and 100 mL 130 g/L ammonium molybdate), 100 g/L ascorbic acid solution, catalyst (the mixture of 200 g potassium sulphate, 6 g copper sulfate pentahydrate and 6 g titanium dioxide), 20 g/L H_3BO_3 solution, mixed indicator (the mixed solution of 0.1 g bromocresol green, 0.02 g methyl red and 100 mL absolute ethyl alcohol), mixed indicator II (the mixed solution of 0.5 g bromocresol green, 0.5 g methyl red and 1000 mL absolute ethyl alcohol) and aqua regia.

The national standard solutions of calcium (Ca) (GSB04-1720-2004), cadmium (Cd) (GSB04-1721-2004), chromium (Cr) (GSB04-1723-2004), copper (Cu) (GSB04-1725-2004), potassium (K) (GSB04-1733-2004), magnesium (Mg) (GSB04-1735-2004), sodium(Na) (GSB04-1738-2004), nickel (Ni) (GSB04-1740-2004), P (GSB04-1741-2004), lead (Pb) (GSB04-1742-2004) and zinc (Zn) (GSB04-1761-2004) were all 1000 μg/mL and obtained from National Center of Analysis and Testing for Nonferrous Metals and Electronic Materials.

The certified reference material (CRM) GBW07408 (GSS-8) was acquired from the Institute of Geophysical and Geochemical Exploration, Chinese Academy of Geological Sciences (Langfang, China).

2.3. Instrumentation

Samples were triturated by a planetary ball mill (QM-3SP4, Laibu, China), weighed with an electronic balance (ATY124, Shimadzu, Japan) and heated in a muffle furnace (KBF1400, Laibu, China). Oscillator (HY-8A, Jingda, China) was used to extract the soluble state of elements in the samples. Centrifuge (TDL-5A, Biaonuo, China) was used to separate the solid from the liquid in the soil suspension. Graphite digester (SPB 50-48, PerkinElmer, America) was applied to the Cu, Pb, Zn, Ni, Cr and Cd digestion. Dispelling furnace (KDNX-20, Leici, China) was used for N digestion. K, Ca, Na and Mg elements were determined by atomic absorption spectrometer (AAS) (A3, Persee, China). The element contents of Cu, Pb, Zn, Ni, Cd and Cr were measured by inductively coupled plasma mass spectrometer (ICP-MS) (Nexion 350D, PerkinElmer, America). The P content was tested by ultraviolet visible spectrometer (UVS) (T6, Persee, China). The functional groups in the samples were determined by fourier transform infrared spectrometer (FTIRS) (Nicolet IS10, Thermo, America). The X-ray diffractometer (XRD) (XD6, Persee, China) was used to measure mineral composition. The sample pH values were determined by pH meter (PHBJ-260, Leici, China). The optimum operating parameters of the AAS and ICP-MS were summarized in Table 1.

2.4. Experimental procedure

The contents of nutrient elements and heavy metals and pH values in saline soil, reference soil and sediment were determined through a series of experiments. Based on these data, different mixing ratios (1:1, 2:1, 5:1, 10:1) of saline-alkali soil and sediment by theoretical calculations were proposed and compared with the reference soil. Then, the restoration of saline-alkali soil was completed by adding the sediment in proportion, which would improve the nutrient composition and soil structure, make the physical and chemical properties of

Table 1 Instrument operating parameters.

ICP-MS		AAS				
Parameter	Setting	Parameter	Setting			
Power	1150 W	Element	K	Ca	Na	Mg
Sampling cone aperture	1.2 mm	Wavelength	766.5 nm	422.7 nm	589.0 nm	285.2 nm
Intercepting cone aperture	1.0 mm	Spectral bandwidth	2.0 nm	0.4 nm	0.4 nm	0.4 nm
Cooling gas flow	18 L/min	Lamp current	2.0 mA	3.0 mA	6.0 mA	2.0 mA
Auxiliary flow	1.2 L/min	Filter coefficient	1	0.6	0.6	0.6
Atomizer flow	0.86 L/min	Integration time	3.0 s	3.0 s	3.0 s	3.0 s
Scan times	20	Burner height	5 mm	6 mm	5 mm	6 mm
Measuring time	60 s	Flame type	Air-C_2H_2	Air-C_2H_2	Air-C_2H_2	Air-C_2H_2

ICP-MS: inductively coupled plasma mass spectrometer; AAS: atomic absorption spectrometer.

the modified saline-alkali soil close to the reference soil and enhance its production capacity. Furthermore, the mineral composition and functional group characteristics of the ameliorated soils with different ratios of sediment and saline-alkali soil (1:1, 2:1, 5:1 and 10:1) were measured and compared, and crop planting experiments were carried out on various ameliorated soils to explore the optimal addition ratio of sediment.

2.4.1. Determination of sample pH

The sample pH was measured in a 1:5 (w/v) soil–water suspension by the calibrated pH meter.

2.4.2. Determination of total Cd, Cr, Cu, Ni, Pb and Zn

The sample was placed in a porcelain boat and heated in a muffle oven at 650℃ for 4 h. 0.2500 g of ashed sample and 10.00 mL 50 % aqua regia were accurately taken into a graphite digestion tube, shaken well, digested on a graphite digestion-meter, cooled to room temperature and filtered through a 0.45 μm membrane. The resulting solution was applied for the Cd, Cr, Cu, Ni, Pb and Zn test in ICP-MS. Meanwhile, the same method was used for the blank control experiment.

2.4.3. Determination of soluble Cd, Cr, Cu, Ni, Pb, Zn, K, Ca, Na and Mg

10.0000 g of sample and 50.00 mL ultrapure deionized water were accurately added into a beaker, oscillated at 180 rpm for 30 min at room temperature and then filtered. The resulting solution was applied for the Cd, Cr, Cu, Ni, Pb, Zn test in ICP-MS and K, Ca, Na, Mg test in AAS. Meanwhile, the same method was used for the blank control experiment.

2.4.4. Determination of total P

0.2500 g of sample was weighed into a nickel crucible and wetted with a few drops of anhydrous ethanol, then 2.0000 g NaOH was added to spread on the surface of the sample. The crucible was covered, heated in the muffle furnace to 400 ℃ for 15 min, heated up to 640 ℃ for another 15 min, cooled to room temperature and taken out. The melted sample was added with 10 mL ultrapure deionized wate, heated to 80 °C to dissolve, and then transferred to a centrifuge tube together with 10 mL H_2SO_4 solution that washed the crucible three times. After centrifugation at 3500 rpm for 10 min, 3 drops of 2,4-dinitrophenol indicator, 1.00 mL ascorbic acid solution and 2.00 mL molybdate solution were added to the

separated supernatant. After standing for 15 min at room temperature, the resulting solution was applied for the total P test in UVS. Meanwhile, the same method was used for the blank control experiment.

2.4.5. Determination of available P

2.5000 g of sample and 50.00 mL sodium bicarbonate extractant were accurately added into a beaker, oscillated at 180 rpm for 30 min at room temperature and then filtered. Then 10.00 mL extraction solution, 5.00 mL molybdenum-antimony chromogenic agent and 10.00 mL ultrapure deionized water were added into a colorimetric tube. After standing for 30 min, the resulting solution was applied for the available P test in UVS. Meanwhile, the same method was used for the blank control experiment.

2.4.6. Determination of total N

1.0000 g of sample, 4.00 mL H_2SO_4 solution, 0.5000 g NaS_2O_3·$5H_2O$ and 1.1 g catalyst were added into a kjeldahl nitrogen digestion bottle and digested. The digestion solution was added with 20.00 mL NaOH solution and then distilled. The distillate was carried on with 20.00 mL H_3BO_3 solution and 3 drops of mixed indicator I, and titrated with a standard solution of HCl to obtain the total N content. Meanwhile, the same method was used for the blank control experiment.

2.4.7. Determination of hydrolysable N

3.0000 g sample and 1.0000 g $FeSO_4$·$7H_2O$ were homogeneously mixed in a distillation tube, added with 50.00 mL ultrapure deionized water and 40.00 mL NaOH solution and then distilled. The distillate was carried on with 30.00 mL H_3BO_3 solution and 5 drops of mixed indicator II, and titrated with a standard solution of HCl to obtain the hydrolysable N content. Meanwhile, the same method was used for the blank control experiment.

3. Results and discussion

3.1. Validation of analytical methods

The calibration curves of Cd, Cr, Cu, Ni, Pb, Zn, K, Ca, Na, Mg and P were established to Table 2 with correlation coefficients all larger than 0.999, revealing that the concentration had a good linear relationship with absorbance or signal strength. According to the requirements of the geological and mineral industry standard DZ/T0011-2015 of the People's

Table 2 Summary for the measurement results of Cd, Cr, Cu, Ni, Pb, Zn, K, Ca, Na, Mg and P in standard solutions.

Element	Concentration (μg/L)	Linear range (μg/L)	Linear equation	R
Cd	0, 1, 2, 3, 4, 5	0–5	$y = 54.107x$	0.9999
Cr	0, 100, 200, 300, 400, 500	0–500	$y = 341.102x$	0.9999
Cu	0, 40, 80, 120, 160, 200	0–200	$y = 138.515x$	0.9999
Ni	0, 40, 80, 120, 160, 200	0–200	$y = 56.907x$	0.9999
Pb	0, 40, 80, 120, 160, 200	0–200	$y = 284.953x$	0.9998
Zn	0, 100, 200, 300, 400, 500	0–500	$y = 255.368x$	0.9999
K	0, 100, 200, 500, 1000, 2000	0–2000	$y = 6.109x - 0.002$	0.9995
Ca	0, 100, 200, 500, 1000, 2000	0–2000	$y = 41.277x + 0.103$	0.9992
Na	0, 100, 200, 500, 1000, 2000	0–2000	$y = 6.261x + 0.056$	0.9991
Mg	0, 100, 200, 500, 1000, 2000	0–2000	$y = 1.307x - 0.019$	0.9993
P	0, 50, 100, 200, 400, 500	0–500	$y = 1.427x + 0.011$	0.9995

R: correlation coefficient.

Republic of China, four parallel measurements of CRM GSS-8 were carried out, and the logarithmic deviation (ΔlgC) and relative standard deviation (RSD) were calculated to verify the accuracy and precision of the analysis methods (Zhao et al., 2020a, 2021). In Table 3, the range of ΔlgC (0.01 %~1.96 %) and RSD (0.28 %~2.94 %) were all lower than the standard monitoring limits, indicating that the accuracy and precision of AAS, ICP-MS and UVS could meet the requirements of geological analysis test. The detection limits were estimated to be three standard deviation (SD) of the blank and in the range of 0.001–0.048 μg/L, hence the experimental methods applied had a high detection capability.

3.2. Comparison of physical and chemical properties of soil

The pH values and major element contents of reference soil, saline-alkali soil and sediment in the study area were respectively measured and shown in Table 4, which were further compared and analyzed in detail.

3.2.1. Sample pH

As can be seen from Table 4, the pH values of reference soil and sediment were separately 6.72 and 6.79, which were both weakly acidic, while the pH value of saline-alkali soil was 9.14, which was strongly alkaline. According to previous studies (He et al., 2020; Zhao et al., 2020b), saline-alkali soil mainly contained high contents of K, Ca, Na and Mg. And the higher the degree of soil alkalization, the higher the content of exchangeable Na in soil. In Table 4, the contents of soluble K and Mg were similar among the three samples, but the Na content in saline-alkali soil was much higher than that in reference soil and sediment, which accorded with the characteristics of high exchangeable Na content in saline-alkali soil. The only difference was that the Ca content in sediment was much higher than that in reference soil and saline-alkali soil, which might be due to the large amounts of fish, shrimp and other aquatic decomposition products in the irrigated area. In general, the contents of K, Ca, Na and Mg in reference soil were basically between that of saline-alkali soil and sediment, which

Table 3 Measurement results of CRM GSS-8.

GSS-8	C_S (μg/g)	C_1 (μg/g)	C_2 (μg/g)	C_3 (μg/g)	C_4 (μg/g)	$\bar{C_i}$(μg/g)	ΔlgC (%)	RSD (%)	DL
Cd	0.130	0.132	0.127	0.128	0.130	0.129	0.25	1.71	0.002 μg/L
Cr	68.000	68.268	67.821	68.149	67.675	67.978	0.01	0.41	0.005 μg/L
Cu	24.300	24.245	24.741	25.061	23.419	24.367	0.12	2.94	0.021 μg/L
Ni	31.500	31.531	31.374	31.467	31.577	31.487	0.02	0.28	0.011 μg/L
Pb	21.000	20.741	21.491	21.167	21.104	21.126	0.26	1.46	0.007 μg/L
Zn	68.000	67.759	68.279	67.591	68.194	67.956	0.03	0.49	0.036 μg/L
K	2.008×10^4	2.027×10^4	2.001×10^4	2.031×10^4	2.047×10^4	2.027×10^4	0.40	0.92	0.003 mg/L
Ca	5.907×10^4	5.771×10^4	5.821×10^4	5.969×10^4	5.746×10^4	5.827×10^4	0.59	1.59	0.007 mg/L
Na	1.269×10^4	1.263×10^4	1.266×10^4	1.273×10^4	1.266×10^4	1.267×10^4	0.05	0.30	0.001 mg/L
Mg	1.428×10^4	1.363×10^4	1.426×10^4	1.342×10^4	1.409×10^4	1.385×10^4	1.33	2.73	0.001 mg/L
P	775.000	779.257	768.594	780.187	764.597	773.159	0.10	1.00	0.048 mg/L

CRM: certified reference material; C_s: national standard value; C_1, C_2, C_3 and C_4: the 1st, 2nd, 3rd and 4th measured value, respectively; $\bar{C_i}$: the average value of four measurements; ΔlgC: logarithmic deviation, $\Delta lgC = \left| lg\,\bar{C_i} - lgC_s \right|$; RSD: relative standard deviation,

$RSD = \frac{\sqrt{\frac{\sum_{i=1}^{n}(C_i - C_s)^2}{n-1}}}{C_s} \times 100\%$, where $n = 4$ was the number of parallel experiments; DL: detection limit.

Table 4 The pH values and major element contents of reference soil, saline-alkali soil and sediment samples.

Sample	Reference soil	Saline-alkali soil	Sediment
pH	6.72	9.14	6.79
Total Cd (μg/g)	1.310	1.482	0.925
Soluble Cd (μg/g)	0.001	0.002	0.006
Total Cr (μg/g)	29.539	26.372	67.621
Soluble Cr (μg/g)	0.209	0.404	0.013
Total Cu (μg/g)	23.149	23.150	36.949
Soluble Cu (μg/g)	0.359	0.617	0.277
Total Ni (μg/g)	13.378	14.278	36.333
Soluble Ni (μg/g)	0.089	0.139	0.362
Total Pb (μg/g)	11.730	11.344	21.441
Soluble Pb (μg/g)	0.043	0.079	0.001
Total Zn (μg/g)	192.348	225.546	281.530
Soluble Zn (μg/g)	0.248	0.366	1.290
Total N (μg/g)	518.420	444.360	740.600
Hydrolysable N (μg/g)	322.000	61.600	513.330
Total P (μg/g)	46.720	5.770	743.300
Available P (μg/g)	18.174	1.072	37.496
Soluble K (μg/g)	85.040	96.190	90.640
Soluble Ca (μg/g)	86.240	21.910	208.855
Soluble Na (μg/g)	50.500	2175.000	87.800
Soluble Mg (μg/g)	45.200	53.050	49.400

indicated that the pH of reference soil was between that of saline-alkali soil and sediment. Therefore, the pH of the saline-alkali soil could be adjusted by adding the sediment to make it close to the reference soil.

3.2.2. Major elements

The main elements in soil refer to the chemical elements necessary for plant growth and development in soil, generally including N, P, K, Ca, Mg, S, Fe, Cu, B, Zn, Mo, Se, Mn, I, Cl and other elements. Although O, C and H are also nutrients needed for plant growth and development, they are mainly supplied by air rather than soil. Na, Si, Co, Ti and so on in soil are important nutrient elements for the growth and development of some but not all plants. According to the different intake of different nutrient elements by plants, they can be classified into macronutrient elements (N, P, K, Ca, Mg, S, etc.) and micronutrient elements (Fe, Mn, B, Zn, Cu, Mo, Cl, etc.). Meanwhile, heavy metal Cu, Pb, Zn, Ni, Cd and Cr are also basic test items in the risk assessment for soil contamination of agricultural land. Therefore, the concentrations of N, P, K, Ca, Na, Mg, Cu, Pb, Zn, Ni, Cd and Cr in the three kinds of samples were determined and analyzed here.

N, P and K, the most important nutrients in soil, can enhance the intensity of plant photosynthesis, increase the rate of sucrose, starch and protein formation, and improve the plant's cold tolerance. The lack of these three elements is detrimental to plant growth and harvest. In Table 4, the P content (total and available) was extremely low and nutrients were thus deficient in saline-alkali soil. In addition, the contents of nutrient elements N and P in saline-alkali soil were lower than those in reference soil, while the N and P contents in sediment were much higher than those in reference soil and saline-alkali soil. Therefore, the addition of sediment in saline-alkali soil could supplement the deficiency of nutrients, increase the soil fertil-

ity, and even ensure the reference growth of crops. However, the K contents in saline-alkali soil, reference soil and sediment were basically the same, which could ensure the supply of nutrients while adjusting the salinity of saline-alkali soil.

Cu, Zn, Ni are essential micronutrient elements for plant growth, but their excess will cause heavy metal pollution in agricultural soil and hinder plant growth. In Table 4, the total contents of Cu, Zn and Ni in saline-alkali land, reference soil and sediment were all lower than the risk screening values for soil contamination of agricultural land in the national standard GB15618-2018 of the People's Republic of China (Table 5). Therefore, the pollution risk of these three elements was low and could be ignored in general. The contents of Cu and Ni in saline-alkali soil and reference soil were basically the same, and lower than those in sediment. The Zn content in both saline-alkali soil and sediment was higher than that in reference soil. Moreover, the soluble contents of Ni and Zn in reference soil were much lower than those of saline-alkali soil and sediment, while the soluble content of Cu in reference soil was between that of saline-alkali soil and sediment. Therefore, the mixing of saline-alkali soil and sediment would not lead to soil heavy metal pollution but provide sufficient micronutrients for plant growth.

Cr, Cd and Pb are highly toxic heavy metals. If their concentrations are too high, they will have negative effects on soil ecology. The total contents of Pb and Cr in saline-alkali land, reference soil and sediment were all lower than the risk screening values for soil contamination of agricultural land in GB15618-2018 (Table 5). Probably as the application of phosphate fertilizer (Carme et al., 2020; Wei et al., 2020), the Cd content was higher than the risk screening value, but lower than the risk intervention value for soil contamination of agricultural land in GB15618-2018. Besides, the soluble contents of the three elements in sediment were extremely low. Therefore, the heavy metal pollution risk of saline-alkali soil, reference soil and sediment used in the experiment was low and could be ignored. The addition of sediment can decrease the soluble contents of these three elements in saline-alkali soil and reduce the potential risk of their migration and transformation to the environment and humans. Meanwhile, the use of fertilizers should be strictly controlled to reduce Cd input into the soil.

Based on the data in Table 4, the theoretical values of the major elements in the ameliorated soil with different proportions (1:1, 2:1, 5:1, 10:1) of saline-alkali soil and sediment were calculated and shown in Table 6. When the mass ratio of saline-alkali soil and sediment (m_s:m_d) was 2:1, the total and soluble amount of heavy metals Cu, Pb and Cd in the amelio-

Table 5 Risk screening value of soil pollution in agricultural land (unit: μg/g).

Pollutant project	Risk screening value	
	6.5 < pH ≤ 7.5	pH > 7.5
Cd	0.3	0.6
Cr	200	250
Cu	100	100
Ni	100	190
Pb	120	170
Zn	250	300

Table 6 Comparison of theoretical and experimental values of major elements in ameliorated soils.

Sample	$T_{1:1}$ (µg/g)	$T_{2:1}$ (µg/g)	$T_{5:1}$ (µg/g)	$T_{10:1}$ (µg/g)	$E_{2:1}$ (µg/g)	Dev (%)	ΔlgC (%)
Total Cd	1.204	1.296	1.389	1.431	1.106	−14.66	6.88
Soluble Cd	0.004	0.003	0.003	0.002	0.001	−66.67	47.71
Total Cr	46.997	40.122	33.247	30.122	32.590	−18.77	9.03
Soluble Cr	0.209	0.274	0.339	0.368	0.258	−5.84	2.61
Total Cu	30.050	27.750	25.450	24.404	26.432	−4.75	2.11
Soluble Cu	0.447	0.504	0.560	0.586	0.549	8.93	3.75
Total Ni	25.306	21.630	17.954	16.283	26.196	21.11	8.32
Soluble Ni	0.251	0.213	0.176	0.159	0.264	23.94	9.32
Total Pb	16.393	14.710	13.027	12.262	12.904	−12.28	5.69
Soluble Pb	0.040	0.053	0.066	0.072	0.066	24.53	9.53
Total Zn	253.538	244.207	234.877	230.635	262.762	7.60	3.18
Soluble Zn	0.828	0.674	0.520	0.450	0.590	−12.46	5.78
Total N	592.480	543.107	493.733	471.291	527.800	−2.82	1.24
Hydrolysable N	287.465	212.177	136.888	102.666	227.867	7.39	3.10
Total P	374.535	251.613	128.692	72.818	235.180	−6.53	2.94
Soluble P	19.284	13.213	7.143	4.383	20.460	54.85	18.99
Soluble K	93.415	94.340	95.265	95.685	89.740	−4.88	2.17
Soluble Ca	115.383	84.225	53.068	38.905	82.040	−2.59	1.14
Soluble Na	1131.400	1479.267	1827.133	1985.255	1296.000	−12.39	5.74
Soluble Mg	51.225	51.833	52.442	52.718	54.800	5.72	2.42

$T_{1:1}$, $T_{2:1}$, $T_{5:1}$ and $T_{10:1}$: theoretical values of the ameliorated soil with the mass ratios (1:1, 2:1, 5:1, 10:1) of saline-alkali soil and sediment, respectively, $E_{2:1}$: experimental value of the ameliorated soil with the mass ratio (2:1) of saline-alkali soil and sediment, Dev: deviation, Dev = $(E_{2:1} − T_{2:1})/T_{2:1}$, ΔlgC: logarithmic deviation, $\Delta lgC = |\Delta lgE_{2:1} − \Delta lgT_{2:1}|$, DL: detection limit.

rated soil was basically the same as that in reference soil. The total amount of Cr was slightly higher than that of reference soil, but the soluble amount was similar to that of reference soil. The total and soluble amount of Zn and Ni were both higher than that of reference soil, making the soil more abundant in micronutrients. The content of K and Mg in the ameliorated soil was similar to that in reference soil, while the content of Ca and Na was higher than that in reference soil, which would ensure the nutrient and water absorption of plant roots in the soil and improve the plant's cold, stress, disease and lodging resistance. In addition, the N content in the ameliorated soil was similar to that in reference soil, and the total amount of P in the ameliorated soil was much higher than that in reference soil, which could promote the movement of sugars in plants and bring more sufficient N and P nutrients to the soil. When $m_s:m_d$ was 1:1, the total amount of Cu, Pb, Cd, Zn and Ni in the ameliorated soil was higher than that in reference soil, while the soluble amount of Cu was lower than that in reference soil, which might prevent the soil from providing sufficient micronutrient elements for plants growth. The Ca content in the ameliorated soil was much higher than that in reference soil, which would lead to the increase of soil pH value, and thus affect the effective absorption of other elements, such as Fe, Zn, Mn, B and Cu. Both the total and soluble amount of P in the soil were too high, which might result in the crops with excessive uptake of P nutrient from the soil, too vigorous respiration, more dry matter consumption than accumulation, early development of reproductive organs, premature maturation, small grains and low yield. When $m_s:m_d$ was 5:1 and 10:1, although the content of heavy metal elements was sufficient, the content of nutrient elements in the ameliorated soil was far lower than that in the reference soil. This would lead to low germination rate, slow growth and stunted of plants, yellowing, drying and even death of leaves. Therefore, in terms of the main element composition in the soil, it

was preliminarily judged that the optimal $m_s:m_d$ was 2:1. The experimental values of the main elements in ameliorated soil with $m_s:m_d$ of 2:1 were tested and listed in Table 6. By comparison, the difference between the theoretical and experimental values were not significant, the content deviation (Dev) and ΔlgC values were about ± 24 % and ± 10 %, respectively. The deviations of soluble Cd were large, which might be due to the low content of element itself. The actual content of soluble P was also higher than the theoretical value, which might be caused by the decrease of soil alkalinity, which increased the solubility of phosphate in the soil. It showed that the theoretical calculation could basically replace the experimental determination to simplify the actual engineering application process.

3.3. Discussion on the optimum ratio of soil remediation

In order to make above mixing ratios of theoretical calculations (1:1, 2:1, 5:1 and 10:1) more convincing, the optimum $m_s:m_d$ was further obtained and proved from the four aspects of soil pH, mineral composition, functional group characteristics, and crop growth.

3.3.1. Soil pH

The pH values of the ameliorated soils were determined by pH meter and listed in Table 7. It was worth noting that the pH value of the ameliorated soil reduced obviously with the

Table 7 The pH values of ameliorated soil samples.

Sample	$m_s:m_d = 1:1$	$m_s:m_d = 2:1$	$m_s:m_d = 5:1$	$m_s:m_d = 10:1$
pH	7.85	7.90	8.27	8.32

increase of sediment addition. In addition, although the pH of the ameliorated soils was reduced, it was still higher than that of the reference soil due to the particularity of the saline-alkali soil in the study area. When the m_s:m_d was 5:1 and 10:1, the soil pH values were both above 8.00. On the contrary, when the m_s:m_d was 1:1 and 2:1, the soil pH values were both below 8.00, and their difference was only 0.05, which was almost negligible. Therefore, under the principle of minimizing the amount of sediment to save costs, the m_s:m_d was recommended to be 2:1.
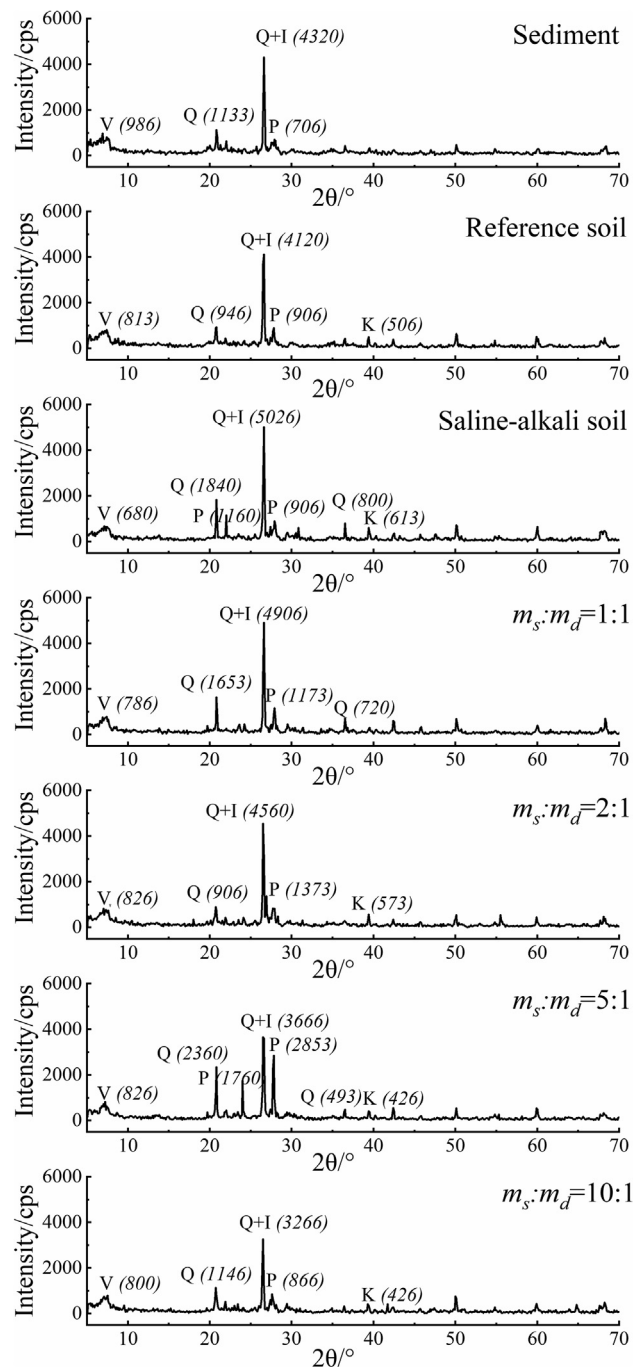
Fig. 2 Comparison of XRD patterns of different samples (V: vermiculite, Q: quartz, I: illite, P: plagioclase, K: kaolinite, Numbers in brackets are the peak height).

3.3.2. Mineral composition

The sediment, reference, saline-alkali and ameliorated soils were scanned by XRD and obtained the spectrogram in Fig. 2. The position of the peak in the XRD spectrum represents different minerals, and the peak height is directly proportional to the mineral content. The XRD peaks appeared in roughly the same places in these soils, but the peak heights were different. This meant that the minerals in these samples were roughly the same in composition, but different in content. Reference soil, sediment and saline-alkali soil all contained a lot of quartz and illite, a little of vermiculite and plagioclase, which might be the main source of alkali metal elements in the three kinds of soil. A small amount of kaolinite was found in reference and saline soils, but almost none in sediments. Judging from the intensity of the diffraction peak, the concentration of quartz, illite, kaolinite and plagioclase in saline-alkali soil was much higher than that in reference soil and sediment. Except for quartz and illite, the content of other minerals was relatively low in sediment, and higher in saline-alkali soil than that in reference soil and sediment. Therefore, the mineral content of ameliorated soil can be adjusted by the different proportion of sediment and saline-alkali soil to make it consistent with that of reference soil.

From the XRD pattern of the ameliorated soil, it could be seen that when the m_s:m_d was 2:1, the diffraction peak intensity of quartz and illite was about 4500, and that of plagioclase was about 1000. The diffraction peak intensity of other minerals was similar to that of minerals in reference soil. When the m_s:m_d was 1:1, the diffraction peak intensity of quartz and illite was about 5000, and that of plagioclase was about 1500, revealing that the contents of quartz, illite and plagioclase in the ameliorated soil were much higher those in the reference soil. Diversely, when the m_s:m_d was 5:1 and 10:1, the diffraction peak intensity of quartz and illite was about 3500, demonstrating that the contents of quartz and illite in the ameliorated soil were much lower than those in the reference soil. In a word, it could also be proved from the perspective of mineral content that the optimal m_s:m_d was 2:1.

3.3.3. Functional group characteristics

The functional group of sediment, reference, saline-alkali and ameliorated soils were detected by FTIRS and presented in Fig. 3. The position of peak in the FTIRS spectrum represents different kinds of functional groups, and the larger the peak area, the higher the content of functional groups. The peaks of these samples appeared at roughly the same locations, indicating that the functional groups of them were roughly the same. But these peaks had different areas, which meant they had different amounts of each functional group. The presence of —OH and Si—O—Si in saline-alkali soil, reference soil and sediment confirmed the presence of kaolinite, illite and quartz. And the content of —OH in the sediment was lower than that in reference soil and saline-alkali soil, indirectly proving that the kaolinite content in the sediment was indeed lower than that in reference soil and saline-alkali soil, which was consistent with the conclusion obtained in Fig. 2. In addition, the content of O=C=O in the sediment was much higher than that in reference soil and saline-alkali soil. The sediment had C=C or C=N, but there were no such functional groups in saline-alkali soil and reference soil. This demonstrated that the content of carbon organic matter in the sediment was more
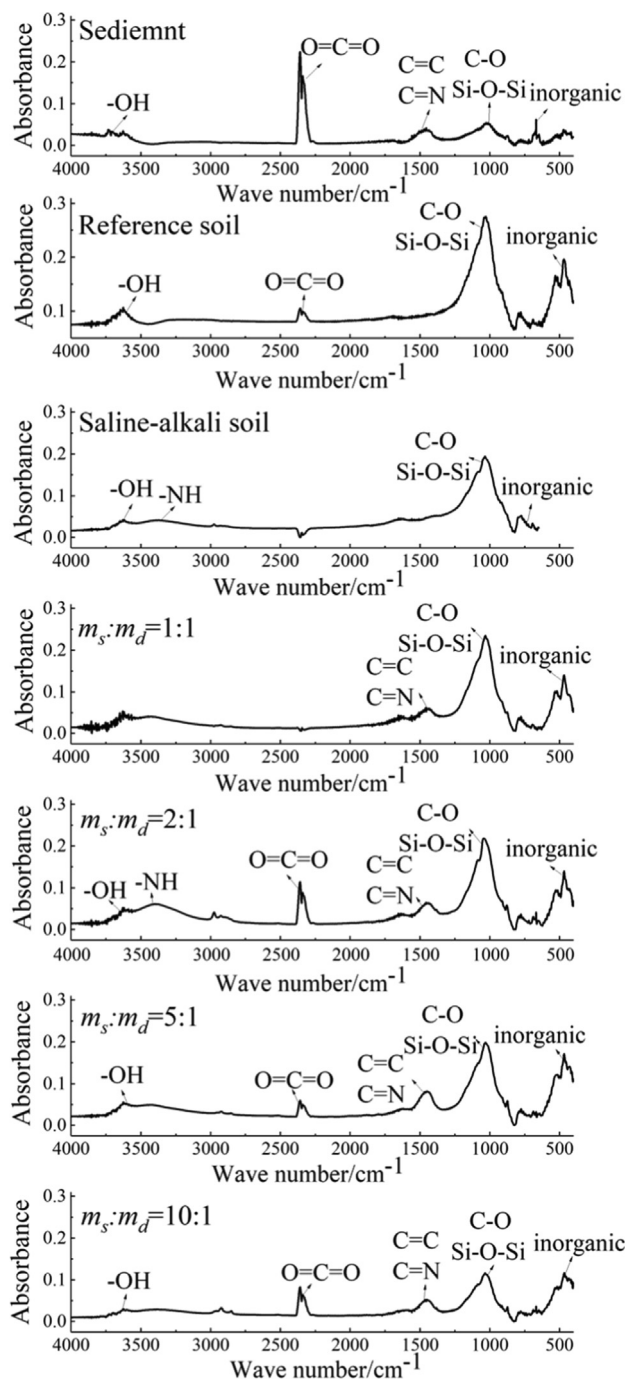
Fig. 3 Comparison of infrared spectrogram of different samples.

abundant than that in reference soil and saline-alkali soil. Moreover, the content of inorganic matter in salinized soil was lower than that in reference soil and sediment.

In Fig. 3, when the $m_s:m_d$ was 2:1, the content of C—O and Si—O—Si in the soil decreased, which meant that the content of quartz and plagioclase in the ameliorated soil decreased. In addition, the content of other carbon-containing functional groups increased. It showed that the content of organic matter in ameliorated soil increased. Meanwhile, the content of other functional groups was close to that of reference soil. When the $m_s:m_d$ was 1:1, the content of C—O, Si—O—Si and inorganic substances in this soil was higher than that in the reference soil

and the ameliorated soil with $m_s:m_d$ of 2:1, indicating a high content of quartz and other minerals in this soil. Conversely, when the $m_s:m_d$ was 5:1 and 10:1, the content of C—O, Si—O—Si and inorganic substances in the two soils was lower than that in the reference soil and the ameliorated soil with $m_s:m_d$ of 2:1, and the content of organic matter (O=C=O, C=C and C=N) was lower than that in the ameliorated soil with $m_s:m_d$ of 2:1. This meant the two soils were low in quartz, other minerals and organic matter. They could not provide enough nutrients for plants to grow. Thus, through the FTIRS diagram of functional groups, the $m_s:m_d$ was further advised to be 2:1.

3.3.4. Crop growth

To verify the practical effect of the improved soil, the spinach planting experiment was carried out in reference soil, saline-alkali soil and four proportions of ameliorated soil. Eight spinach seeds were planted in each soil and watered regularly. After about 1 week, spinach seed germination rate in reference soil and ameliorated soil with $m_s:m_d$ of 1:1 and 2:1 were about 70~80 %. To ensure that the soil can provide adequate nutrients for plant growth, only two plants were kept in each pot. After about 4 weeks, the growth of spinach plants in reference soil and the ameliorated soil with $m_s:m_d$ of 1:1 and 2:1 was shown in Fig. 4a–c. The spinach plants in the $m_s:m_d = 2:1$ ameliorated soil were significantly better than those in the $m_s:m_d = 1:1$ ameliorated soil. In the $m_s:m_d = 2:1$ ameliorated soil, spinach plants were thicker, leaves were larger and basically not yellow, and there was basically no lodging phenomenon. Although the leaves of spinach plants in the $m_s:m_d = 1:1$ ameliorated soil did not turn yellow, the plants were short and lodging. This might be ascribed to high P content in the soil, leading to excessively vigorous respiration of plants, early development of reproductive organs and premature crop maturation. In the saline-alkali soil and ameliorated soils with $m_s:m_d$ of 5:1 and 10:1, the spinach seeds basically did not germinate or the plants were short, as shown in Fig. 4d–f. In addition, applying the same amount of water to the soil in the same time, the reference soil and the ameliorated soils with $m_s:m_d$ of 1:1 and2:1 had better water retention, while the saline-alkali soil and the ameliorated soils with $m_s:m_d$ of 5:1 and 10:1 had poor water retention and were prone to drought. Therefore, according to the plant growth, the optimal $m_s:m_d$ should also be 2:1.

Fig. 4 Comparison of growth situation of spinach in different soils.

3.3.5. Summary of four characteristic indexes

By comparing and analyzing the soil pH, mineral composition, functional group characteristics and crop growth status of sediment, reference, saline-alkali and ameliorated soils, it was found that the saline-alkali soil was hardened and impervious, its pH was greater than 9, and its exchangeable Na content was high. Too high pH caused the imbalance of acid and base in the soil environment, and the large number of Na ions also damaged the pore structure of the soil, resulting in the dynamic imbalance of ions. The lack of carbonaceous organic matter and inorganic carbonate brought about the high content of minerals such as quartz which were not conducive to crop growth. These microscopic characteristics lead to low emergence rate, short stature and difficult survival of plants in saline-alkali soil. The sediment was acidic and rich in organic matter, which could change the loose soil structure, reshape the aggregate structure of the soil, and regulate the physical and chemical properties of the soil. When the $m_s{:}m_d$ was 2:1, the content of organic matter and inorganic carbonate in the ameliorated soil increased significantly, and the pH value also decreased 13.6 %. All indexes were close to the reference soil with sufficient nutrients, and crops could normally germinate, grow and develop in the ameliorated soil. Sampling, analysis, test and simulation calculation should be done again according to local conditions in different regions to obtain the best mixing ratio of saline-alkali soil and sediment. Although the mixing ratio varies with the conditions in different regions, the engineering approach is applicable to the improvement of saline-alkali soil. It expands the idea and method of saline-alkali soil amelioration and is beneficial to reduce the cost.

4. Conclusions

This article reported a method of saline-alkali soil improvement in western Jilin province of northeast China by adding natural sediment of the adjacent irrigated area. The pH values and major element concentrations of sediment, reference and saline-alkali soils were determined and compared. The pH value of saline-alkali soil was greater than 9, it contained a lot of quartz and lacked organic matter, inorganic carbonate and other nutrients. But sediment had rich nutrients and organic matter, which could make up for the shortcomings of saline-alkali soil, that is, it can supplement N, P and other nutrition elements, adjust the salinity, and maintain the stability of trace elements Cu, Zn and other heavy metals. The theoretical values of the major elements in the ameliorated soil with different proportions (1:1, 2:1, 5:1, 10:1) of saline-alkali soil and sediment were calculated, and the optimal $m_s{:}m_d$ was preliminarily judged to be 2:1. Furthermore, a series of experiments (analysis and test of soil pH, mineral composition, functional group composition and crop growth) also revealed that the best $m_s{:}m_d$ was 2:1, that is, in the $m_s{:}m_d = 2{:}1$ ameliorated soil, the pH decreased and the nutrient elements and trace elements were sufficient, which could guarantee the germination and growth of plants. However, with different soil characteristics in different regions, the mixing ratio would be different.

This saline-alkaline soil amelioration method made full use of the surrounding natural waste and had the advantage of adapting measures to local condition, low cost, high efficiency and environmental friendliness. At the same time, the theoretical calculation could basically replace the batch experiment to simplify the actual engineering application process. The study was comprehensive and provided a new idea for the amelioration and restoration of saline-alkali land.

References

Amini, S., Ghadiri, H., Chen, C., Marschner, P., 2016. Salt-affected soils, reclamation, carbon dynamics, and biochar: a review. J. Soils Sediments 16 (3), 939–953. https://doi.org/10.1007/s11368-015-1293-1.

Bao, S.C., Wang, Q., Bao, X.H., Li, M., Wang, Z.J., 2016. Biological treatment of saline-alkali soil by sulfur-oxidizing bacteria. Bioengineered 7 (5), 372–375. https://doi.org/10.1080/21655979.2016.1226664.

Bian, J.M., Jie, T., Zhang, L.S., Ma, H.Y., Zhao, J., 2012. Arsenic distribution and geological factors in the western Jilin province, China. J. Geochem. Explor. 112, 347–356. https://doi.org/10.1016/j.gexplo.2011.10.003.

Bouwer, H., 2000. Integrated water management: emerging issues and challenges. Agr. Water Manage. 45 (3), 217–228. https://doi.org/10.1016/S0378-3774(00)00092-5.

Carme, G., Leconte, S., Sirot, V., Breysse, V., Badot, P.M., Bispo, A., Deportes, I.Z., Dumat, C., Rivièrea, G., Crépeta, A., 2020. Mass balance approach to assess the impact of cadmium decrease in mineral phosphate fertilizers on health risk: the case-study of French agricultural soils. Sci. Total Environ. 760,. https://doi.org/10.1016/j.scitotenv.2020.143374 143374.

Evgeny, A., Aleksei, L., Mikhail, A., Wang, W.J., Ji, X.W., 2021. The influence of brown and south polar skua on the content of plant nutrient in the soils from the Fildes Peninsula (King George Island, West Antarctica). Chem. Ecol. 37 (2), 185–199. https://doi.org/10.1080/02757540.2020.1839435.

Fu, R.M., Chang, H.P., Zhu, M.F., Chen, W.L., 2018. Research, application demonstration of key technology for microbial remediation of saline-alkali soil. Int. J. Agric. Biol. 20 (11), 2556–2560. https://doi.org/10.17957/IJAB/15.0821.

Ge, Y., Cheng, Z.Y., Hu, J., Sun, F.R., Yang, J.W., 2018. Regulation of saline-alkali barrier in coastal saline-alkali land of Jiangsu Province under different straw utilization methods. Jiangsu Agr. Sci. 46 (2), 223–227. https://doi.org/10.15889/j.issn.1002-1302.2018.02.056.

Guo, Z.B., Yan, G.J., Zhang, R.H., Li, F.M., Zeng, Z.X., Liu, H., 2010. Improvement of soil physical properties and aggregate-associated C, N, and P after cropland was converted to grassland in semiarid loess plateau. Soil Sci. 175 (2), 99–104. https://doi.org/10.1097/SS.0b013e3181cda54a.

He, K., He, G., Wang, C.P., Zhang, H.P., Xu, Y., Wang, S.M., Kong, Y.Z., Zhou, G.K., Hu, R.B., 2020. Biochar amendment ameliorates soil properties and promotes Miscanthus growth in a coastal saline-alkali soil. Appl. Soil Ecol. 155,. https://doi.org/10.1016/j.apsoil.2020.103674 103674.

Jonathan, P.S., Chris, K., Brendan, C., Dariush, M., Yue, H., Piotr, B., Simon, C., Laurie, W., Parke, W., Martin, O.F., Renata, M.,

2018. Estimating the health and economic effects of the proposed US Food and Drug Administration voluntary sodium reformulation: microsimulation cost-effectiveness analysis. PLoS Med. 15 (4), 1–18. https://doi.org/10.1371/journal.pmed.1002551.

Kuzmin, A.I., Tusupbekov, Z.A., Ryapolova, N.L., Nadtochiy, V.S., 2020. Environmental improvement of saline and alkali soils in the kamyshlovskay revival a valley and of natural grassland efficiency. IOP Conf. Ser.: Mater. Sci. Eng. 941,. https://doi.org/10.1088/1757-899X/941/1/012011 012011.

Li, F.Z., Huang, Z.B., Ma, Y., Sun, Z.J., 2018. Improvement effects of different environmental materials on coastal saline-alkali soil in yellow river delta. Mater. Sci. Forum. 913 (1), 879–886. https://doi.org/10.4028/www.scientific.net/MSF.913.879.

Li, S., Yang, Y.C., Li, Y.C., Gao, B., Tang, Y.F., Xie, J.Z., Zhao, H.C., 2020. Remediation of saline-sodic soil using organic and inorganic amendments: physical, chemical, and enzyme activity properties. J. Soils Sediments 20 (3), 1454–1467. https://doi.org/10.1007/s11368-019-02510-4.

Mao, W.B., Kang, S.Z., Wan, Y.S., Sun, Y.X., Li, X.H., Wang, Y.F., 2016. Yellow river sediment as a soil amendment for amelioration of saline land in the yellow river delta. Land Degrad. Dev. 27 (6), 1595–1602. https://doi.org/10.1002/ldr.2323.

Pu, L.M., Zhang, S.W., Li, F., Wang, R.H., Yang, J.C., Chang, L.P., 2018. Impact of farmland change on soybean production potential in recent 40 years: a case study in Western Jilin, China. Int. J. Environ. Res. Public Health. 15 (7), 1522. https://doi.org/10.3390/ijerph15071522.

Qadir, M., Tubeileh, A., Akhtar, J., Larbi, A., Minhas, P.S., Khan, M.A., 2008. Productivity enhancement of salt-affected environments through crop diversification. Land Degrad. Dev. 19 (4), 429–453. https://doi.org/10.1002/ldr.853.

Rahneshan, Z., Nasibi, F., Moghadam, A.A., 2018. Effects of salinity stress on some growth, physiological, biochemical parameters and nutrients in two pistachio (Pistacia vera L.) rootstocks. J. Plant Interact. 13 (1), 73–82. https://doi.org/10.1080/17429145.2018.1424355.

Schuiling, R.D., 1990. Geochemical engineering: some thoughts on a new research field. Appl. Geochem. 5 (3), 251–262. https://doi.org/10.1016/0883-2927(90)90001-L.

Schuiling, R.D., 1998. Geochemical engineering; taking stock. J. Geochem. Explor. 62 (1), 1–28. https://doi.org/10.1016/S0375-6742(97)00042-3.

Wang, Z.Q., 1993. Chinese Saline Soil. Science, Beijing.

Wang, J.L., Feng, W.Z., Zhang, H., Sun, J., Zhao, Q.L., 2021a. Experimental study on the effect of deep pine technology on water and salt transport in soda saline land. Arabian J. Geosci. 14 (7), 1–10. https://doi.org/10.1007/s12517-021-06893-y.

Wang, Z.Y., Tan, W.J., Yang, D.Q., Zhang, K.Q., Zhao, L.W., Xie, Z.G., Xu, T., Zhao, Y.W., Wang, X.N., Pan, X.L., Zhang, D.Y., 2021b. Mitigation of soil salinization and alkalization by bacterium-induced inhibition of evaporation and salt crystallization. Sci. Total Environ. 755, (part 1). https://doi.org/10.1016/j.scitotenv.2020.142511 142511.

Wang, Z.J., Zhuang, J.J., Zhao, A.P., Li, X.X., 2018. Types, harms and improvement of saline soil in Songnen Plain. IOP Conf. Ser.: Mater. Sci. Eng. 322, (5). https://doi.org/10.1088/1757-899X/322/5/052059 052059.

Wei, B.G., Yu, J.P., Cao, Z.Q., Meng, M., Yang, L.S., Chen, Q., 2020. The availability and accumulation of heavy metals in greenhouse soils associated with intensive fertilizer application. Int. J. Environ.

Res. Public Health 17 (15), 53–59. https://doi.org/10.3390/ijerph17155359.

Wong, V.N.L., Greene, R.S.B., Dalal, R.C., Murphy, B.W., 2010. Soil carbon dynamics in saline and sodic soils: a review. Soil Use Manage. 26 (1), 2–11. https://doi.org/10.1111/j.1475-2743.2009.00251.x.

Wu, C.B., 2002. Geochemical engineering: an environmental protection industry in 21 century. Geophys, Geochem, Explor. 26 (6), 411–414. https://doi.org/10.3969/j.issn.1000-8918.2002.06.001.

Yang, C.X., Liu, Y.J., Zhao, W.N., Wang, N., 2021a. Colonization Characteristics and diversity of arbuscular mycorrhizal fungi in the rhizosphere of Iris lactea in Songnen saline-alkaline grassland. Phyton 90 (3), 719–729. https://doi.org/10.32604/phyton.2021.015024.

Yang, H.J., Xia, J.B., Cui, Q., Liu, J.T., Wei, S.C., Feng, L., Dong, K.K., 2021b. Effects of different Tamarix chinensis-grass patterns on the soil quality of coastal saline soil in the Yellow River Delta China. Sci. Total Environ. 772,. https://doi.org/10.1016/j.scitotenv.2021.145501 145501.

Yang, Y.Y., Zhang, S.W., Wang, D.Y., Yang, J.C., Xing, X.S., 2014. Spatiotemporal changes of farming-pastoral ecotone in Northern China, 1954–2005: a case study in Zhenlai County, Jilin Province. Sustainability 7 (1), 1–22. https://doi.org/10.3390/su7010001.

Yang, H., Zhang, P., Zhu, T.B., Li, Q., Cao, J.H., 2019. The characteristics of soil C, N, and P stoichiometric ratios as affected by geological background in a Karst Graben Area, Southwest China. Forests 10 (7), 601. https://doi.org/10.3390/f10070601.

Zhang, Y.J., Chu, G.H., Dong, P., Xiao, J., Meng, Q., Baumgartel, M., Xu, B., Hao, T., 2018. Enhanced electrokinetic remediation of lead- and cadmium-contaminated paddy soil by composite electrolyte of sodium chloride and citric acid. J Soils Sediments 18 (5), 1915–1924. https://doi.org/10.1007/s11368-017-1890-2.

Zhang, G.X., Wei, D., Yang, Y.S., Salama, R.B., 2010. Evolution study of a regional groundwater system using hydrochemistry and stable isotopes in Songnen Plain, northeast China. Hydrol. Processes 21 (8), 1055–1065. https://doi.org/10.1002/hyp.6286.

Zhao, Y.Y., Li, H., Li, B., Lai, Y.W., Zang, L.B., Tang, X.D., 2021. Process design and validation of a new mixed eluent for leaching Cd, Cr, Pb, Cu, Ni, and Zn from heavy metal-polluted soil. Anal. Methods 13 (10), 1269–1277. https://doi.org/10.1039/d0ay01978j.

Zhao, Y.G., Wang, S.J., Li, Y., Liu, J., Zhuo, Y.Q., Chen, H.X., Wang, J., Xu, L.Z., Sun, Z.T., 2018. Extensive reclamation of saline-sodic soils with flue gas desulfurization gypsum on the Songnen Plain, Northeast China. Geoderma 321 (1), 52–60. https://doi.org/10.1016/j.geoderma.2018.01.033.

Zhao, Y.Y., Zhang, Z.Y., Li, B., Zhao, Y., Lu, J.L., Tang, X.D., 2020a. Accurate determination and comprehensive evaluation of heavy metals in different soils from Jilin Province in Northeast China. Anal. Lett. 54 (12), 1901–1928. https://doi.org/10.1080/00032719.2020.1828908.

Zhao, W., Zhou, Q., Tian, Z.Z., Cui, Y.T., Liang, Y., Wang, H.Y., 2020b. Apply biochar to ameliorate soda saline-alkali land, improve soil function and increase corn nutrient availability in the Songnen Plain. Sci. Total Environ. 722,. https://doi.org/10.1016/j.scitotenv.2020.137428 137428.

Zhu, T.S., Shao, T.Y., Liu, J.Y., Li, N., Long, X.H., Gao, X.M., Zed, R., 2021. Improvement of physico-chemical properties and microbiome in different salinity soils by incorporating Jerusalem artichoke residues. Appl. Soil Ecol. 158,. https://doi.org/10.1016/j.apsoil.2020.103791 103791.